Rotating toroidal nuclei

Cheuk-Yin Wong

Oak Ridge National Laboratory, * *Oak Ridge, Tennessee 37830*

For very rapidly rotating nuclei, the moment of inertia can be readily increased if the mass is distributed in the form of a torus. Thus, a rotating toroid can be a figure of equilibrium when the angular momentum exceeds a certain limit. The angular momentum thresholds for the onset of toroidal figures of equilibrium are evaluated and found to be greater than the limits at which the fission barriers vanish for nuclei with the topology of a sphere. Stability against sausage deformation, in which the toroid becomes thicker in some sections but thinner in some other, is examined. We obtain two different results on the question of stability, depending on the flow pattern in the presence of these axially asymmetric deformations which, in turn, is greatly affected by the dissipative mechanism.

> NUCLEAR STRUCTURE Rotating toroidal nuclei. Nuclei with very large angu-
> lar momentum. Sausage stability. Regions of stable rotating toroidal nuclei.

I. INTRODUCTION

The equilibrium shape of a nucleus under rotation has been the subject of many investigations. From the survey of Cohen, Plasil, and Swiatecki,[1] we know how in the liquid-drop model the equilibrium shapes vary with the angular momentum and the fissility parameter. Additional nuclear shell effects sometimes alter the equilibrium shapes.[2] Furthermore, as the classical-type treatment in terms of a mechanical system can only be of use in describing the average behavior of a quantal system, statistical fluctuations of the actual energies from the classical mean may have very peculiar consequences such as the possibility of the existence of yrast traps put forth by Bohr and Mottelson.[3]

Recent measurements of the total fusion cross section in heavy-ion reactions suggest that the liquid-drop limit of critical momentum at which the fission barrier vanishes for a nucleus with the topology of a sphere has been exceeded[4] while a different measurement reaches this limit.[5] If one takes into account the competition of particle emission, the critical angular momentum should be defined as the angular momentum at which the fission barrier height is of the order of the binding energy of the least bound particle. Seen in this light, reaching the so-called "liquid-drop limit" is, in fact, exceeding the proper limit for stability against fission for a nucleus with the topology of a sphere. The breakdown of such a limit can, of course, be explained in terms of dynamical effects, the details of which are still rather obscure, or in terms of changes of liquid-drop parameters. On the other hand, one can raise the pertinent question whether the so-called liquid-drop limit is the

only limit for all shapes. What if the shapes are drastically different from that of a sphere?

As of yet, much of the discussion of a rotating nucleus is limited to shapes with the topology of a sphere. However, for very rapidly rotating systems, the moment of inertia can be readily increased if the mass is distributed in the form of a torus. Equilibrium or quasiequilibrium toroidal systems become possible.[6] Indeed, many rapidly rotating and gravitating toroidal objects have been observed.[7] There is even the interesting suggestion that the mass distribution (as distinct from the visible light distribution) of our nearest neighboring galaxy, the Andromeda, is essentially toroidal.[8] The fact that some rapidly rotating systems have been observed to be toroidal and the apparent breakdown of the liquid-drop limit for a nucleus with the topology of a sphere calls for a careful examination of the stability of rotating toroidal nuclei.

In this first survey of the rotating toroidal nuclei, we shall focus our attention on the treatment of these nuclei as classical mechanical systems endowed with a uniform charge density and a surface tension. The interesting consequences, if any, due to the shell effects can be dealt with as in Ref. 9 but will not be treated here.

In Sec. II we consider toroidal nuclei in equilibrium and observe that as the angular momentum exceeds a certain limit, there can be toroidal figures of equilibrium. In Sec. III we examine the stability (or instability) of the rotating toroidal nuclei under "sausage" deformations in which the toroid becomes thicker in some sections and thinner in some others. We obtain two different results on the question of stability, depending on the flow pattern in the presence of these axially asym-

metric sausage deformations, which, in turn, is greatly affected by the dissipative mechanism. In Sec. IV we discuss the fate of the rotating toroidal nuclei under the most optimistic estimates of sausage stability so as to provide characteristics for their detection, if they ever live long enough to become detectable.

II. ROTATING TOROIDAL NUCLEI IN EQUILIBRIUM

In the discussion of rotating toroidal nuclei in equilibrium we shall restrict ourselves to cases where the fluid elements are in a uniform rotation about the symmetry axis with a common angular velocity. Such a motion is also called rigid-body rotation as the velocity field and the moment of inertia are the same as those of a rotating rigid body. Our restriction is a natural one. For, in a classical mechanical system, viscous forces can transfer the necessary angular momentum point by point and dissipate the necessary energies to convert a nonuniform rotation to a uniform rotation, given a sufficient lapse of time. Secondly, the rotating energy of a rapidly rotating nucleus in the nuclear cranking model is what one obtains in a uniform rotation, when angular momentum is sufficiently large such that the nuclear pairing force becomes ineffective.[10] Of course, one does not wish to imply that the current flow inside a nucleus in the cranking model is a uniform one (as a matter of fact, recent investigations[11] suggest the opposite); the uniform rotation can be used here to calculate the rotational energy of a rapidly rotating nucleus.

As in the case of a rotating and gravitating mass, one knows very well that the meridian of a rotating toroidal nucleus in perfect equilibrium is not circular. In the gravitational case, self-consistent figures of equilibrium were calculated.[6] The meridian of the equilibrium figure is found to be nearly elliptical with the "major axis" lying perpendicular to the direction of the central symmetry axis of the torus.[6] So, with the Coulomb repulsion, the meridian of the figure of equilibrium is expected to be nearly elliptical with the "major axis" lying in the same direction as the central symmetry axis. For the evaluation of the equilibrium shape, one can follow the self-consistent treatment presented in Ref. 6. However, such a treatment is rather complicated and does not seem to be warranted at the present time. Furthermore, the action of the surface tension is expected to counterbalance the long-range Coulomb repulsion in reducing the ellipticity which can therefore be neglected in the first approximation. Hence, we consider the simple case of a toroidal nucleus whose meridian is restricted to be circular. Such

a problem lends itself to a simple treatment in toroidal coordinates in terms of which analytic expressions for various relevant quantities are already known.[9]

A toroidal nucleus having a circular meridian is characterized by a major radius R measured from the geometrical center of the torus to the center of the meridian and a minor radius d which is the radius of the circular meridian. The ratio of the major to minor radius R/d is defined as the aspect ratio of the torus. In toroidal coordinates, the surface with such an aspect ratio is the coordinate η:

$$\eta = \cosh^{-1}(R/d) . \tag{2.1}$$

For a deformation which preserves axial symmetry and the volume of the nucleus and a rotation about the symmetry axis, the energy of the nucleus as a function of η is given by

$$E(N,Z,\eta) = E_s^{(0)}(N,Z)g_s(\eta) + E_C^{(0)}(N,Z)g_C(\eta)$$
$$+ E_r^{(0)}(N,Z)g_r(\eta) , \tag{2.2}$$

where $E_s^{(0)}$ and $E_C^{(0)}$ are the surface and Coulomb energies of a spherical nucleus with the same volume, while $E_r^{(0)}$ is the rotational energy for the spherical nucleus having the same angular momentum. In terms of the parameters for the liquid-drop mass formula, the surface, Coulomb, and rotational energies are:

$$E_s^{(0)}(N,Z) = a_2 \left[1 - \kappa_s \left(\frac{N-Z}{A} \right)^2 \right] A^{2/3} , \tag{2.3}$$

$$E_C^{(0)}(N,Z) = C_3 Z^2 / A^{1/3} , \tag{2.4}$$

$$E_r^{(0)}(N,Z) = L^2 / \tfrac{2}{5}(m_n r_0^2 A^{5/3}) , \tag{2.5}$$

where a_2 is the surface energy coefficient, $\kappa_s a_2$ is the surface symmetry energy, C_8 is the Coulomb energy coefficient, m_n is the nucleonic mass, and r_0 is the radius parameter. The surface geometric factor $g_s(\eta)$ is[9]

$$g_s(\eta) = (4\pi \cosh\eta/9)^{1/3}. \tag{2.6}$$

The Coulomb geometrical factor $g_C(\eta)$ is[9]

$$g_C(\eta) = \frac{5}{6}\left(\frac{3\pi}{2\cosh^2\eta}\right)^{1/3}\frac{\sinh^5\eta}{\cosh\eta}$$

$$\times \left[\frac{8}{9\pi^3}\sum_{n=0}^{\infty}\epsilon_n \mathcal{B}_n(\cosh\eta)\mathcal{C}_n(\cosh\eta)\right.$$

$$\left. - \frac{1}{8\pi}\frac{\cosh\eta}{\sinh^5\eta}(4\cosh^2\eta+3)\right] , \tag{2.7}$$

where ϵ_n is the Neumann factor defined by

$$\epsilon_n = 1 \quad \text{for } n = 0$$

$$= 2 \quad \text{for } n = 1, 2, 3, \ldots$$

The functions $\mathcal{B}_n$ and $\mathcal{C}_n$ are

$$\mathcal{B}_n(\cosh\eta) = (n+\tfrac{1}{2})P_{n+\frac{1}{2}}(\cosh\eta)Q_{n-\frac{1}{2}}^{\ 2}(\cosh\eta)$$
$$- (n-\tfrac{3}{2})P_{n-\frac{1}{2}}(\cosh\eta)Q_{n+\frac{1}{2}}^{\ 2}(\cosh\eta) \quad (2.8)$$

$$\mathcal{C}_n(\cosh\eta) = (n+\tfrac{1}{2})Q_{n+\frac{1}{2}}(\cosh\eta)$$
$$- (n-\tfrac{3}{2})Q_{n-\frac{1}{2}}(\cosh\eta)Q_{n+\frac{1}{2}}^{\ 2}(\cosh\eta) , \quad (2.9)$$

where the functions P_n^m and Q_n^m are Legendre functions of the first and second kind with order n degree m (toroidal harmonics). The geometrical factor for a rigid-body rotation about the symmetry axis is[6]

$$g_r(\eta) = \frac{8}{5}\left(\frac{2}{3\pi\cosh\eta}\right)^{-2/3}(4\cosh^2\eta + 3)^{-1}. \quad (2.10)$$

The geometrical factors as a function of the aspect ratio R/d are given in Fig. 1. One observes that g_C is a monotonically decreasing function of the aspect ratio R/d.[12] The function g_C has a magnitude less than unity, indicating a smaller magnitude of the electrostatic energy as compared with that of an equivalent spherical nucleus with the same volume. The rotational geometrical fac-
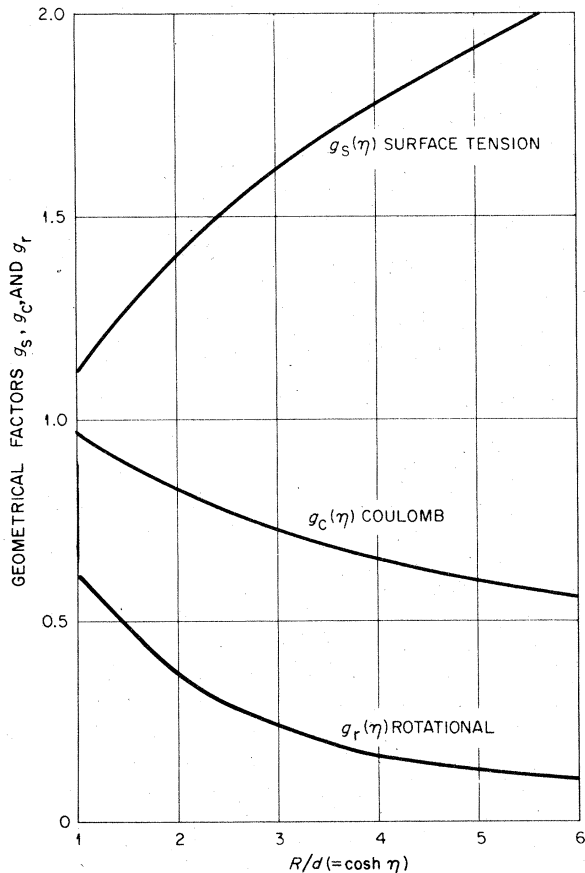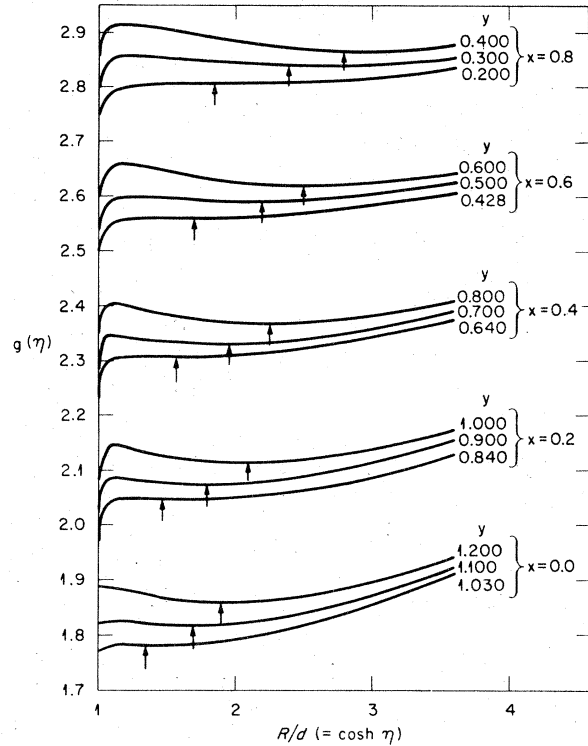

FIG. 2. Total geometrical factor as a function of the toroidal aspect ratio R/d. For each value of x, the lower curve gives the threshold of the rotational parameter at which a toroidal minimum just begins to develop. The other two curves are the total geometrical factor for higher values of the rotational parameter y. The positions of the energy minima are indicated by arrows.

tor g_r is a monotonically decreasing function of the aspect ratio, while the surface tension geometrical factor g_s is a monotonically increasing function of the aspect ratio.

It is of interest to note that in the region $1.0 \lesssim R/d \lesssim 2.0$, the magnitudes of the slopes of g_r with respect to R/d are approximately twice as large as the corresponding slopes of $g_C(\eta)$. We shall see how such an approximate relationship affects the boundary of the threshold of toroidal rotating nuclei.

We introduce the dimensionless measure of Coulomb and rotational energies as in Ref 1:

$$x = E_C^{(0)}/2E_s^{(0)} , \quad (2.11)$$

$$y = E_r^{(0)}/E_s^{(0)} , \quad (2.12)$$

where x is the usual fissility parameter and y is the rotational parameter. Then, the deformation energy can be written in terms of the surface energy and the total geometrical factor g:

$$E(N,Z,\eta) = E_s^{(0)}(N,Z)g(\eta) , \quad (2.13)$$

where

FIG. 1. Geometrical factors as a function of the toroidal aspect ratio R/d.

$$g(\eta) = g_s(\eta) + 2x\,g_c(\eta) + y\,g_r(\eta) \,. \tag{2.14}$$

With these definitions, the deformation energy (apart from the scale of $E_s^{(0)}$) is determined entirely by $g(\eta)$. An examination of this total geometrical factor $g(\eta)$ then reveals stability or instability against variations of η (or the aspect ratio R/d).

The total deformation energy of toroidal nuclei with different fissility parameters and rotational parameters can be easily calculated from the different geometrical factors. As the surface tensional geometrical factor is a monotonically increasing function of the aspect ratio while the Coulomb and the rotational geometrical factor is a monotonically decreasing function of the aspect ratio, it is clear that there can be an energy minimum in the η degree of freedom when the fissility parameter and the rotational parameter exceeds a certain limit.

We show in Fig. 2 the total geometrical factor as a function of the aspect ratio for selected combinations of x and y parameters. For each value of x, the lowest curve is the total geometrical factor for the particular threshold value of y at which the toroidal minimum begins to develop. After the toroidal minimum is developed, an increase in angular momentum gives rise to an increase in the aspect ratio. The positions of the minima are indicated by arrows.

As the value of x increases, the values of y at which toroidal energy minima begin to develop decreases. We plot in Fig. 3 the boundary in the (x,y) plan for the toroidal threshold above which toroidal equilibria are possible. It is of interest to note that the boundary is given approximately by the equation

$$x + y \cong 1. \tag{2.15}$$

Such a result is a consequence of the fact that the magnitude of the slopes of the geometrical factor g_r is about twice that of g_c in the region $1.0 \lesssim R/d \lesssim 2.0$ where the energy minima are first located. As the equilibrium condition is obtained by

$$\frac{\partial g}{\partial \eta} = 0 \,, \tag{2.16}$$

the approximate relation between the slopes allows one to write down the following approximate equilibrium condition:

$$\frac{\partial g_s}{d\eta} + 2(x+y)\,\frac{\partial g_c}{\partial \eta} \simeq 0. \tag{2.17}$$

On the other hand, we know[9] that a toroidal nucleus without rotation begins to have an energy minimum when $x \simeq 1$, we see from Eq. (2.17) that the inclusion of rotation leads to the approximate relation
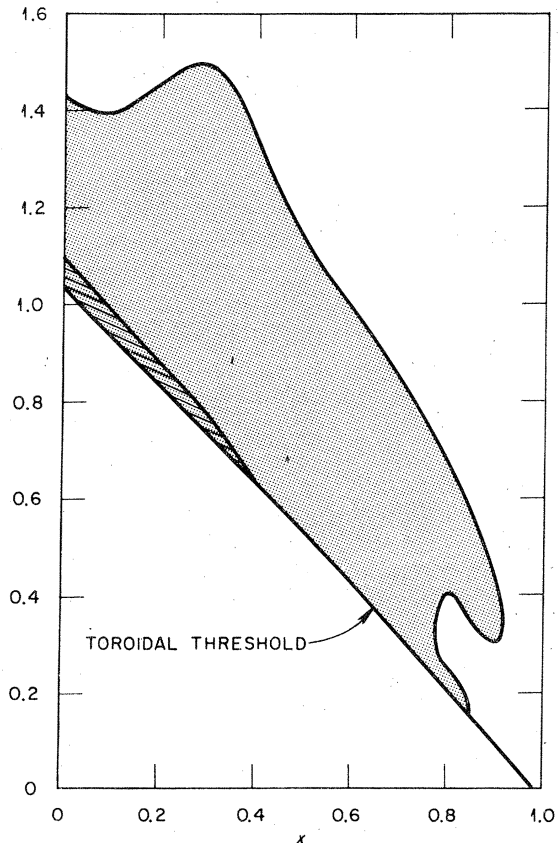

FIG. 3. The solid line is the toroidal threshold above which toroidal energy minima develop. The hatched region is the stable region if the nucleus maintains rigid-body rotation in the presence of sausage deformations, while the shaded region is the stable toroidal region if an axially asymmetric flow follows a sausage deformation (see Sec. III).

TABLE I. Threshold rotating parameters y, beyond which toroidal minima develop, are listed as a function of the fissility parameter x. Given also are the aspect ratios R/d, total geometrical factor g, and the relative geometrical factor ξ for these threshold cases.

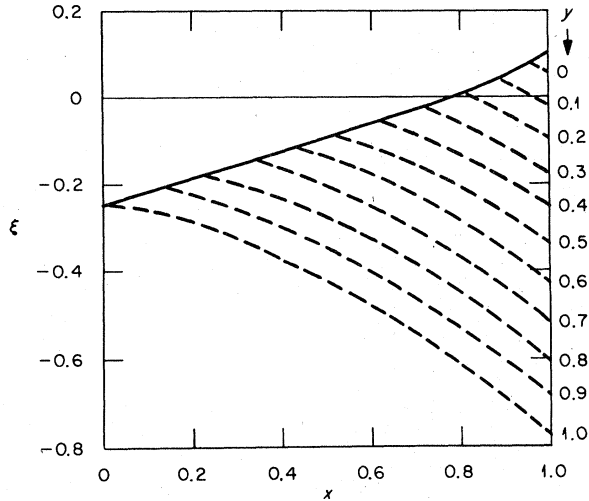| x	y	R/d	g	ξ
0	1.030	1.375	1.785	−0.2449
0.1	0.938	1.462	1.919	−0.2192
0.2	0.840	1.471	2.049	−0.1906
0.3	0.742	1.550	2.180	−0.1619
0.4	0.640	1.577	2.399	−0.1313
0.5	0.536	1.655	2.436	−0.0996
0.6	0.428	1.700	2.562	−0.0658
0.7	0.316	1.761	2.686	−0.0298
0.8	0.200	1.850	2.809	0.0085
0.9	0.080	1.970	2.929	0.049 18
0.964	0.000	2.079	2.005	0.0771

FIG. 4. The total geometrical factor of the toroidal minimum relative to that of a sphere for various combinations of x and y values. Each dotted curve is the result for a single y value. The solid curve is the envelope for the toroidal thresholds.

(2.15) for the onset of toroidal minima.

As a function of x, the threshold rotational parameters are listed in Table I, together with the equilibrium aspect ratios and total geometrical factors. As is observed, the aspect ratios for the threshold increases with fissility parameters, indicating that the Coulomb repulsion is effective in pushing the major radius outward.

For a given value of x, one finds that the threshold value of y for a toroidal equilibrium exceeds the rotational parameter for the fission barrier to vanish.[1] It appears that the toroidal sequence is not connected with the sequences of shapes involved in those with the topology of a sphere.

The geometrical factor of a toroidal minimum can be expressed relative to the geometrical factor for a spherical nucleus with the same volume and angular momentum:

$$\xi = g - (1 + 2x + y).$$

We plot the relative geometrical factor ξ as a function of x and y in Fig. 4. As is observed, when a toroidal equilibrium configuration is possible, the relative geometrical factor is negative, except for $x \gtrsim 0.78$ and for small values of y. Thus, for these nuclei with negative values of ξ, the total energies of the toroidal minima are lower than the corresponding energies for the spherical shape.

III. SAUSAGE DISTORTIONS

In our previous analysis of a nonrotating toroidal nucleus, sausage instability is found to be the most important instability of the toroidal nucleus. For a rotating toroidal nucleus, a rigorous treatment of stability against axially asymmetric sausage distortions necessitates a complete hydrodynamical analysis, as the perturbation of the shape will, in general, be associated with a nonuniform perturbation of the flow. We shall defer such a dynamical treatment until a later date and content ourselves with quasistatic properties in simple cases, where the flow patterns under sausage distortions are assumed known. Our treatment follows closely our previous analysis of a gravitating toroidal mass (where following Dyson[13] the term "beaded displacement" is used instead of the term "sausage distortion" or "sausage deformation").

The surface shape of a toroidal nucleus having sausage deformations σ_λ about an equilibrium shape $\eta = \eta_0$ is given by

$$\eta = \eta_0 \left(1 + \sigma_0 + \sum_{\lambda=1} \sigma_\lambda \cos\lambda\phi \right) , \tag{3.1}$$

where λ is the number of maxima (or minima) of the meridian area and σ_0 is of the order of σ_λ^2 and is introduced to conserve volume under sausage deformation.

With a density confined to the boundary as given by Eq. (3.1), the Coulomb energy and the surface energies, when expressed in powers up to σ^2, can be written as

$$E_C(\eta, \sigma) = E_C^{(0)} \left[g_C(\eta) + \frac{1}{2} \sum_{\lambda=1} C_\lambda \sigma_\lambda^2 \right] \tag{3.2}$$

and

$$E_s(\eta, \sigma) = E_s^{(0)} \left[g_s(\eta) + \frac{1}{2} \sum_{\lambda=1} s_\lambda \sigma_\lambda^2 \right] , \tag{3.3}$$

where the coefficients C_λ and s_λ have been calculated previously.[9]

The moment of inertia for rotation about the axis through the center of mass can also be separated into two parts[6]:

$$I(\eta, \sigma) = I^{(0)} \left/ \left[g_r(\eta) + \frac{1}{2} \sum_{\lambda=1}^{\infty} r_\lambda \sigma_\lambda^2 \right] \right. , \tag{3.4}$$

where

$$r_\lambda = - d_\lambda / g_r^2 \tag{3.5}$$

and

$$d_\lambda = \frac{5}{8} \left(\frac{2}{3\pi \cosh\eta} \right)^{2/3} \frac{\eta^2}{\sinh^2\eta}$$

$$\times \left[(8\cosh^4\eta + 64\cosh^2\eta + 33) \right.$$

$$\left. - 2(8\cosh^4\eta + 24\cosh^2\eta + 3)\frac{3\coth^2\eta - 2}{3\coth^2\eta - 1} \right]$$

$$- \delta_{\lambda 1} \frac{5}{4} \eta^2 \sinh^6\eta(-3 + 5\coth^2\eta)^2 , \tag{3.6}$$

where we have taken into account the shift of center of mass for a sausage deformation of order $\lambda = 1$.

In the presence of dissipation, viscous forces can transfer the necessary angular momentum point by point and dissipate the necessary energies to convert a nonuniform rotation into a uniform rotation, after a certain lapse of time. How rapid such a conversion can take place is completely unknown. We shall consider two limiting cases. First, we consider the case where the viscous force is so strong as to convert a nonuniform rotation into a uniform rotation almost instantaneously so that a uniform angular velocity is approximately maintained under a sausage deformation. Secondly, we consider the case where viscous forces are hardly operative so that an axially asymmetric flow follows an axially asymmetric sausage distortion, being faster at a constriction and slower at a bulge.

A. Rigid-body rotating under sausage distortions

In the presence of a viscous force strong enough to maintain approximately a rigid-body rotation under sausage deformation, the coefficients C_λ, s_λ, and r_λ determine the question of stability. The rotational energy becomes

$$E_r = E_r^{(0)}\left[g_r(\eta_0) + \frac{1}{2}\sum_{\lambda=1}^{\infty} r_\lambda \sigma_\lambda^2 \right] \qquad (3.7)$$

and the total energy of the system under this assumption is

$$E = E_s^{(0)}\left[g_s(\eta_0) + 2x g_c(\eta_0) + y g_r(\eta_0) \right.$$

$$\left. + \frac{1}{2}\sum_\lambda K_\lambda \sigma_\lambda^2 \right], \qquad (3.8)$$

where

$$K_\lambda = s_\lambda + 2x C_\lambda + y r_\lambda. \qquad (3.9)$$

Thus, in this case, the sign of K_λ determines stability or instability. In Fig. 5, we plot the stability coefficients r_λ as a function of the aspect ratio. The other coefficients s_λ and C_λ have been presented previously in Fig. 5 of Ref. 7 and will not be reproduced here. One observes[9] that s_1 is always negative while s_λ for $\lambda \geq 2$ is positive for $R/d \lesssim \lambda$ and negative thereafter. On the other hand, C_1 is always positive while C_λ for $\lambda \geq 2$ is negative for $R/d \lesssim \lambda$ and positive thereafter. The values of r_λ are the same for all λ values if rotation is about the geometrical axis. A correction for the shift of center of mass gives r_1 different from the other r_λ's. As one observes, r_1 is positive always while the other r_λ's are positive for $R/d \geq 1.5$.

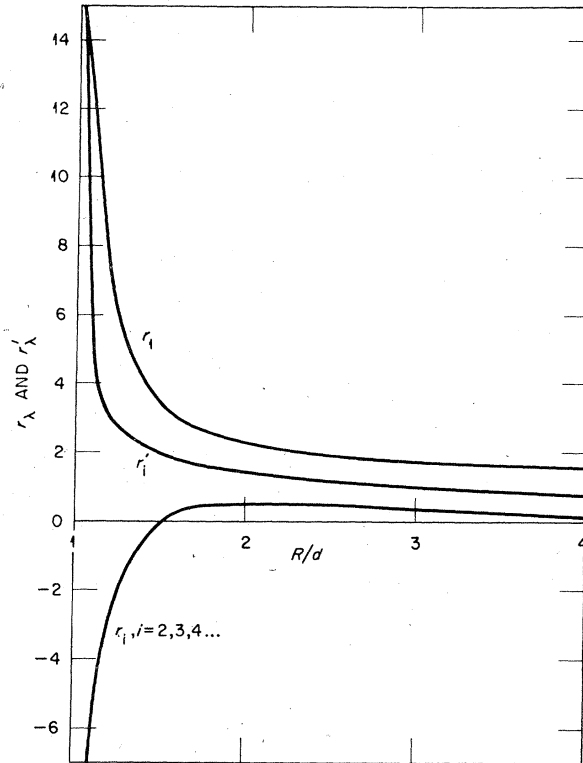We evaluate the total stability constant K_λ for the

FIG. 5. The rotational stability coefficients as a function of the aspect ratio. The curves labeled r_1, r_i where $i = 2, 3, 4, \ldots$ are the coefficients of rotational stability under the assumption of a uniform rotation in the presence of sausage deformations, while the curve labeled r_i' is the coefficient of stability under the assumption of axially asymmetric flow in the presence of sausage deformations.

threshold of toroidal equilibrium. That is, for a given value of x, we evaluate K_λ for the values of rotational parameter y and the aspect ratio R/d listed in Table I. Out of such a calculation we obtain the stability constant K_λ for various values of x at the toroidal threshold. They are plotted in Fig. 6. One observes that under the assumption of rigid-body rotation in the presence of sausage deformation, the incipient rotating toroidal nucleus is stable for distortions of all orders when $x \lesssim 0.41$. When x exceeds ~ 0.41, it remains stable against distortions of order $\lambda = 1$, 3, 4, and 5 but becomes unstable against distortions of order $\lambda = 2$. As a sausage instability of order $\lambda = 2$ leads eventually to a disintegration into two equal pieces, the fate of incipient rigidly rotating toroidal nuclei with $x \gtrsim 0.41$ is a toroidal breakup of two equal fragments.

The stability constants K_λ plotted in Fig. 6 are evaluated for the incipient rotating toroidal nucleus. As the rotational parameter y increases
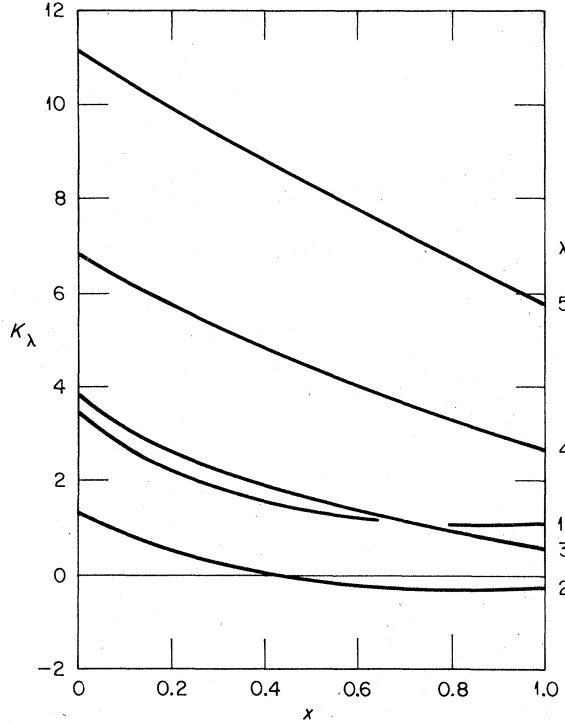
FIG. 6. Total coefficients of stability K_λ for nuclei at the toroidal threshold as a function of the fissility parameter for sausage deformations of various orders.

above the threshold values, these curves will move downward. Such a downward movement arises because of the shift to a greater aspect ratio as y increases. The rapid decrease of the stability constant s_λ with respect to an increase in the aspect ratio results in greater sausage instability as the rotational parameter y increases. Thus, we have the following order in which instability sets in: first, there is the instability of order $\lambda = 2$, followed by $\lambda = 3$ and $\lambda = 1$ which occur quite close to each other, and then $\lambda = 4$ and 5. The region of stability, after sausage distortion of all orders is considered, is shown as the cross-hatched region in Fig. 3. As one observes, the region of stability is very small indeed. In terms of angular momentum, the stable region encompasses only a few units of $\hbar$. It appears therefore that in the presence of dissipative forces such that rigid-body rotation is maintained throughout sausage distortions, a rotating toroidal nucleus is unstable against sausage distortions for all intents and purposes.

B. Non-rigid-body rotation under sausage deformation

As mentioned previously, an axially asymmetric distortion of the torus will generally lead to axially

asymmetric patterns of flow. The assumption of rigid-body rotation discussed in Sec. III A is an idealization in the presence of frictional forces transferring the necessary angular momentum point by point and dissipating the necessary energy. What of other forms of flow pattern which are not axially symmetric and where the viscous force is inoperative? We can follow the method of Dyson[13] and discuss a simple case with the axially asymmetric flow pattern. Under sausage deformations, the area of the meridians becomes a function of the azimuthal angle. As the nuclear fluid can be considered incompressible, in order to maintain the same mass flow across different meridians, the flow velocity needs to depend on the area of the meridian. It is faster at a constriction and slower at a bulge. The average velocity $v(\phi)$ for the meridian at ϕ is then a function of ϕ:

$$v(\phi) = v_0 A_0 / A(\phi) , \qquad (3.10)$$

where A is the area of the meridian at the azimuthal angle ϕ and A_0 and v_0 are the area and the average velocity of the meridian without sausage deformation. The dependence of the meridian area on the surface toroidal coordinate $\eta_s(\phi)$ leads from Eq. (3.10) to

$$v(\phi) = v_0 \sinh^2 \eta_0 / \sinh^2 \eta_s(\phi) . \qquad (3.11)$$

In consequence, the kinetic energy under sausage distortion is related to the rotational kinetic energy without sausage distortion $E_r^{(0)} g_r(\eta_0)$ by

$$E_r = E_r^{(0)} \left[g_r(\eta_0) + \sum_{\lambda=1} r_\lambda' \sigma_\lambda^2 \right] , \qquad (3.12)$$

where

$$r_\lambda' = g_r(\eta_0) \eta_0 \left[1 + \frac{3 \coth^2 \eta_0 - 2}{3 \coth^2 \eta_0 - 1} (\coth^2 \eta_0 + 1) \right] \qquad (3.13)$$

and the stability constant K_λ becomes

$$K_\lambda = s_\lambda + 2x C_\lambda + y r_\lambda' . \qquad (3.14)$$

The coefficient r_λ' is now independent of the order of sausage distortion. In Fig. 5 we plot r_λ' as a function of the aspect ratio. As is observed, it is always a positive quantity and it decreases as the aspect ratio increases. The pattern of flow under the present assumption of Dyson has the effect of stabilizing the sausage distortions.

With the knowledge of the r_λ' coefficients, we can calculate the coefficient of stability K_λ for various values of x, y at the equilibrium toroidal aspect ratio. One then obtains the region of stability as the shaded region given in Fig. 3 in the x-y plane. We observe that for nuclei up to $x \sim 0.85$, there are regions of rotational parameters in which a
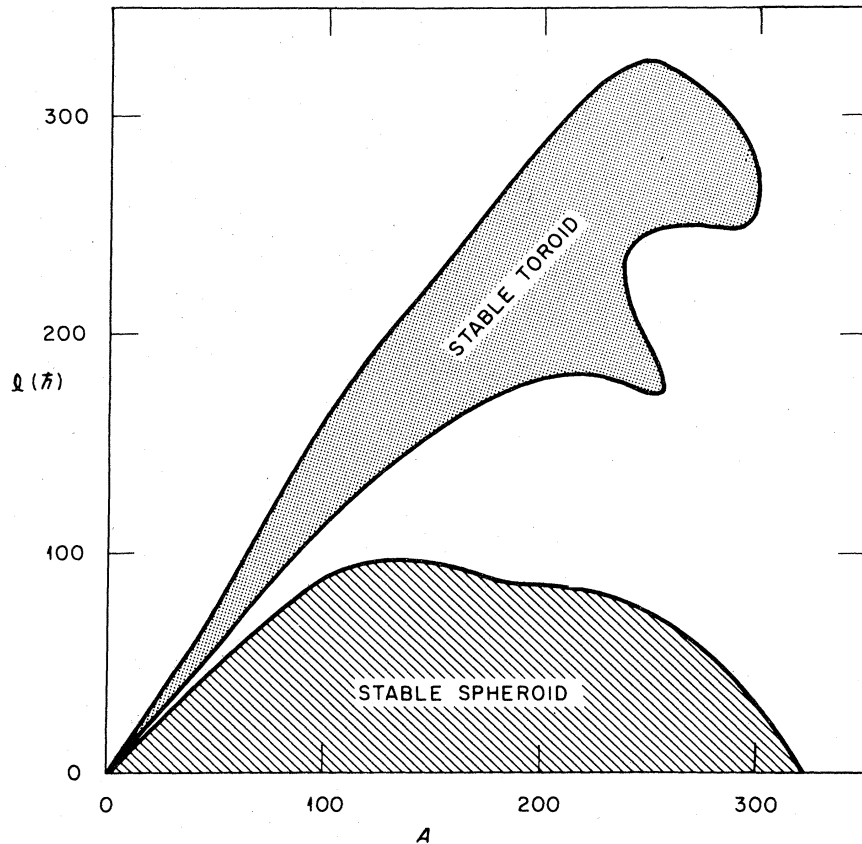
FIG. 7. Stable toroidal region in the plane of angular momentum l and mass number A for nuclei along the β-stability line.

toroidal rotating nucleus is stable against sausage distortions with the axially asymmetric flow pattern of Dyson.

For different values of x, the instability which sets in at $y \geq y_{max}$ is of a different type. This is understandable as the aspect ratio is usually smaller for smaller values of x and y, and the smaller aspect ratio is usually associated with sausage instability of lower order. For $x \lesssim 0.2$, it is the $\lambda = 1$ sausage instability which provides a limit to the rotational parameter and for $0.2 \lesssim x \leq 0.7$ the sausage instability of order $\lambda = 2$ provides a limit to y_{max}. For $x \sim 0.8$ and x slightly greater than 0.8, sausage instability of order $\lambda = 2$ sets a limit of y_{max} for $y \sim 0.24$, while sausage instability of order $\lambda = 3$ sets up the limit of y_{max} for $y \sim 0.7$.

So far, the region of stability is given in the x, y plane for convenience. It is of practical interest to express the stability region in terms of angular momenta l and mass number A. Using the mass formula of Myers and Swiatecki,[14] we obtain from Fig. 3 the stable toroidal region in the l-A plane for nuclei along the β-stability line (Fig. 7). As is observed, the region of stability is quite

large under the present assumption of the pattern of axially asymmetric flow given by Dyson. The angular momentum even reaches a value up to $l \sim 300 \ \hbar$.

IV. DISCUSSION

From the analysis of the last section, we have two very different results for the stability of the rotating toroidal nuclei, depending on the flow pattern in the presence of sausage deformations which in turn is greatly affected by the dissipative mechanism.

However unlikely it may seem, it is of interest to obtain information on the rotating toroidal nuclei under the most optimistic estimates of sausage stability in order to provide characteristics for their detection, if they ever live long enough to become detectable. For this reason, we shall discuss the fate of rotating toroidal nuclei in the stable toroidal region of Fig. 7, keeping in mind the restrictive nature of our assumptions with regard to the flow pattern. How these nuclei come into being is a separate question which need not concern us

TABLE II. The transition energies ΔE for an $E2$ transition in a toroidal nucleus along the β-stability line. The toroidal nuclei with angular momentum between l_{min} and l_{max} are stable against sausage deformations, on the assumption of an axially asymmetric flow following a sausage deformation. Here, $\Delta E(l_{min})$ and $\Delta E(l_{max})$ are, respectively, the transition energies at l_{min} and l_{max}; x is the fissility parameter, and Z and A are the charge and mass numbers of the nucleus on the β-stability line.

x	Z	A	l_{min}	$\Delta E(l_{min})$ (MeV)	l_{max}	$\Delta E(l_{max})$ (MeV)
0.1	11	23.9	25.33	10.85	30.95	7.89
0.2	22.4	50.5	56.92	7.057	74.26	4.80
0.3	34.2	79.4	90.22	4.99	127.86	3.32
0.4	46.3	110.5	122.40	3.87	177.12	2.55
0.5	58.6	143.4	150.71	2.96	217.86	2.04
0.6	71.0	178.1	172.21	2.31	261.91	1.64
0.7	83.5	214.3	182.28	1.73	304.18	1.35
0.8	96.0	251.9	173.71	1.20	190.30	1.10
0.8	96.0	251.9	248.75	1.06	324.99	1.07
0.9	121.3	291.0	249.83	0.77	292.04	0.81

here.

Consider first a "cold" rotating toroidal nucleus. Although these nuclei may be stable against sausage deformations and particle emission, they are unstable against γ decays. We envisage the deexcitation of the rotating toroidal nuclei by γ radiation with a multipolarity of 2 and an energy given by

$$\Delta E(l) = E(l) - E(l-2) = 4yg_r E_s^{(0)}/l ,$$

where g_r is the rotational geometrical factor evaluated at the equilibrium aspect ratio appropriate for the angular momentum l. This γ energy is characterized by a larger moment of inertia as compared with that with spherical topology and therefore is typically lower than that for the same spherical nuclei with the same angular momentum. The γ-ray energy is given in Table II for the maximum and the minimum l values in the stable region of Fig. 7. There may be yrast traps either due to the nuclear shell effects or statistical fluctuations.[3] Without the occurrence of these traps, γ deexcitation will bring the nuclei to the toroidal threshold below which a toroidal equilibrium is

impossible. At this juncture, the nucleus may tunnel through a barrier in the η degree freedom to change the topology from toroidal to ellipsoidal. The accompanying change of topology, which may be slightly delayed, brings the nucleus to an ellipsoidal shape with a rotational parameter exceeding that of the Cohen, Plasil, and Swiatecki limit for the fission barrier to vanish. The nucleus will subsequently undergo fission. The examination of the γ-ray energies before the fission of the toroidal nucleus, if experimentally feasible, will provide information on the intermediate toroidal configuration.

With regard to the liquid-drop angular momentum limit and the heavy-ion total fusion cross section which partly motivated the present investigation, our result indicates that there can be a different limit of angular momentum when the shape of the nucleus is drastically different from that of a sphere. However, our result as it is does not explain how the liquid-drop limit of a sphere can be exceeded. Our stable toroidal region is not connected to the stable spheroidal region of Cohen, Plasil, and Swiatecki. Consequently, after the toroidal threshold is reached and conversion to a spheroid takes place, the resultant spheroidal nucleus has an angular momentum exceeding the limit for a spheroidal nucleus and will subsequently fission. The present result, however, has the restriction on the circular shape of the meridian, which is not a truly self-consistent equilibrium shape, particularly near the toroidal threshold. Removal of such a restriction may perhaps modify the toroidal threshold to bring it within the region of stable spheroidal nuclei for $A < 100$. This, however, remains to be studied. If the toroidal and spheroidal regions have an overlap, our conclusion on the fate of toroidal nuclei mentioned in the last paragraph needs to be modified.

A more definitive analysis of sausage stability calls for a complete hydrodynamical analysis of the flow. In this respect, the nuclear hydrodynamical computer program we have developed[15] for the investigation of heavy-ion collisions can be easily adopted for such an investigation in the future.

[1]S. Cohen, F. Plasil, and W. J. Swiatecki, Ann. Phys. (N.Y.) 82, 557 (1974).
[2]R. Bengtsson, S. E. Larsson, G. Leander, P. Möller, S. G. Nilsson, S. Åberg, and Z. Symanski, Lund report (unpublished).
[3]A. Bohr and B. R. Mottelson, Phys. Scr. 10A, 13 (1974).
[4]M. N. Namboodiri, E. T. Chulick, J. B. Natowitz, and R. A. Kenefick, Phys. Rev. C 11, 401 (1975).
[5]R. G. Stokstad, R. A. Dayras, J. Gomez del Campo, and P. H. Stelson, ORNL report (unpublished).
[6]C. Y. Wong, Astrophys. J. 190, 675 (1974).

[7]J. Theys and E. A. Spiegel, Astrophys. J. 208, 650 (1976); 212, 616 (1977).

[8]H. Arp, Astrophys. J. 139, 1045 (1963); B. F. Burke, K. C. Turner, and M. A. Tuve, Carnegie Yearbook 63, 341 (1964); M. S. Roberts, in *Proceedings of the International Astronomical Union Symposium No. 31*, edited by H. Van Woerden (Academic, New York, 1967), p. 189; V. C. Rubin and W. K. Ford, Astrophys. J. 159, 379 (1970).

[9]C. Y. Wong, Ann. Phys. (N.Y.) 77, 279 (1973).

[10]A. Bohr and B. R. Mottelson, *Nuclear Structure* (Benjamin, New York, 1975), Vol. II.

[11]M. Radomski, Phys. Rev. C 14, 1704 (1976).

[12]The present result differs from our previous result of the Coulomb geometrical factor only at the point $R/d = 1$. The singular behavior in Coulomb energy and C_λ at $R/d = 1.0$ obtained previously in Ref. 9 is due to the use of insufficient terms in the numerical summation of this series in Eq. (2.7) for this particular point. When the proper limit is taken, or when a sufficient number of terms are included, the singular behavior disappears. The author is indebted to Dr. Bonnie Miller for calling attention to such an error. As the point $R/d = 1$ plays no role in the discussion of stability of toroidal systems, the discrepancy at just this point does not affect the results obtained previously in Refs. 6 and 9.

[13]F. W. Dyson, Phil. Trans. Roy. Soc. 184, 43 (1892).

[14]W. D. Myers and W. J. Swiatecki, Ark. Fys. 36, 343 (1967).

[15]H. H. K. Tang and C. Y. Wong, Bull. Am. Phys. Soc. 22, 645 (1977).